Investigation of Electromagnetic Pulse Welding for the Automated Production of Resource-Efficient Multi-Material Joints

S. O. Kraus[1*], M. Graß[2], J. Bruder[1], C. Pabst[3], J. Holz[4], J. Wiedemann[5], S. Frodl[6], M. Heckmann[7], P. Frint[8], S. Böhm[2], P. Groche[1]

[1] Institute for Production Engineering and Forming Machines, TU Darmstadt, Germany
[2] Department for Cutting and Joining Manufacturing Processes, Institute of Production Technology and Logistics, University of Kassel, Germany
[3] PSTproducts GmbH, Germany
[4] Chemische Werke Kluthe GmbH, Germany
[5] Constellium Singen GmbH, Germany
[6] inTec automation GmbH, Germany
[7] LÄPPLE AUTOMOTIVE GmbH, Germany
[8] Nordmetall GmbH, Germany
*Corresponding author. Email: stefan.kraus@ptu.tu-darmstadt.de

Abstract

Electromagnetic pulse welding (EMPW) is a promising technology for the automated production of multi-material joints made of high-strength aluminium alloys and steels and is therefore capable of realising light-weight design by exploiting the potential of both materials. The ongoing Design2Collide research project is investigating the potential applications of EMPW in an industrial environment with the aim of reducing the limitations associated with the use of the process. Its automation capability is demonstrated by converting a state-of-the-art robotic production cell to join a demonstration assembly made of steel (DC04) and aluminium (AA6016). Welding studies to derive process windows with the best joint strengths are carried out using an EMPW system and a special model test rig for collision welding. Reproducible attainment of ample joint strength is indicated by failure of the base material AA6016 due to shearing, while the joint itself remains intact. To ensure excellent joint properties, an in-line quality control method based on active thermography is developed and integrated into the automated process. Initial stand-alone tests of the developed method with the EMPW system show promising results for feasibility and industrial qualification. The examination of the EMPW value chain is currently being

completed by the investigation of corrosion prevention and passivation systems for the pre- and post-treatment of materials and their impact on weldability, and by the improvement of process simulation. For the latter, adapted material models are essential. Respective flow curves have already been determined for the materials used at high strain rates of up to 10^4 1/s.

Keywords

Electromagnetic Pulse Welding, Multi-Material Design, Lightweight Concepts, Emission Reduction

1 Introduction

The transport sector accounts for about 21% of global CO_2 emissions, with passenger cars contributing about 38% of this share (Crippa et al., 2024; EDGAR, 2024; IEA, 2025). In addition to greenhouse gases, non-exhaust particulate emissions - especially from tyre wear and brake dust - are gaining attention as they are strongly influenced by vehicle weight (Lopez et al., 2023; OECD, 2017; Timmers et al., 2016). Reducing vehicle mass therefore helps to reduce both CO_2 emissions and particulate pollution such as microplastics (Bandivadekar et al., 2008; Beddows and Harrison, 2021; OECD, 2017). Lightweight design using multi-material design, particularly high-strength steel and aluminium, plays a key role in this effort (Tisza & Lukács, 2018).

However, joining these dissimilar materials remains a challenge. Conventional fusion welding methods, such as laser or TIG welding, often lead to the formation of brittle intermetallic phases due to different melting points, which significantly reduce the strength of the joint (Agudo et al., 2007; Atabaki et al., 2014; Carlone and Astarita, 2019; Khedr et al., 2023). As a solid-state or collision welding process, electromagnetic pulse welding (EMPW) offers a promising alternative (Agudo et al., 2007; Kapil and Sharma, 2015; Khedr et al., 2023). Currently, EMPW process design relies on iterative methods, which are costly and introduce uncertainties in mass production (Marschner et al., 2021).

The ongoing Design2Collide research project is investigating the potential applications of EMPW in an industrial environment with the aim of reducing the limitations associated with the use of the process. The entire chain for integrating the joining technology into industrial series production of multi-material components made of aluminium and steel materials is being analysed. Welding tests are carried out using an EMPW system and a special model test rig for collision welding to determine process windows and parameters with the best possible joint strength. These two systems are also used to implement measures to improve quality and extend process limits by investigating corrosion prevention and passivation systems for the pre- and post-treatment of materials and their impact on weldability. This machine-level approach will also be used to develop an in-line quality control method for subsequent integration into automated EMPW production processes. The

automation of the EMPW process will be achieved by converting a robotic production cell for joining a demonstration assembly made of steel (DC04) and aluminium (AA6016).

In parallel to the physical processes and investigations mentioned above, the EMPW process is also being analysed and further developed on the level of numerical simulation. For this purpose, adapted material models are required. Corresponding flow curves have already been determined for the materials used in the project at high strain rates of up to 10^4 1/s. The numerical representation of the collision process and the associated prediction of the joint formation will thus enable the simulation-based design and stress analysis of EMPW joined components in the future. The knowledge gained in the course of the project, both at the real process level and at the simulation level, will finally be transferred to the production of an EMPW Crash Management System (CMS) for passenger cars. The design of the EMPW-CMS will be adapted compared to a conventionally manufactured CMS in order to enable EMPW-compatible production on the one hand, and to make best use of the lightweight concepts and strength potential resulting from the EMPW technology in combination with high-strength aluminium and steel materials on the other hand.

In the following sections, this paper discusses the process and the process steps carried out in the project to adapt and qualify the robotic production cell and the demonstration assembly, both originally designed for conventional joining processes, for automated EMPW production.

2 Methodological structure

The structure of the Design2Collide research project shown in Fig. 1 is divided into the physical process research track and the process simulation track. At the end of the project, knowledge from both areas will be transferred to the production of the EMPW Crash Management System. In the following sections, this paper presents the physical process research and the path to automated EMPW production of an established component. In Fig. 1, these are the top three boxes on the left.

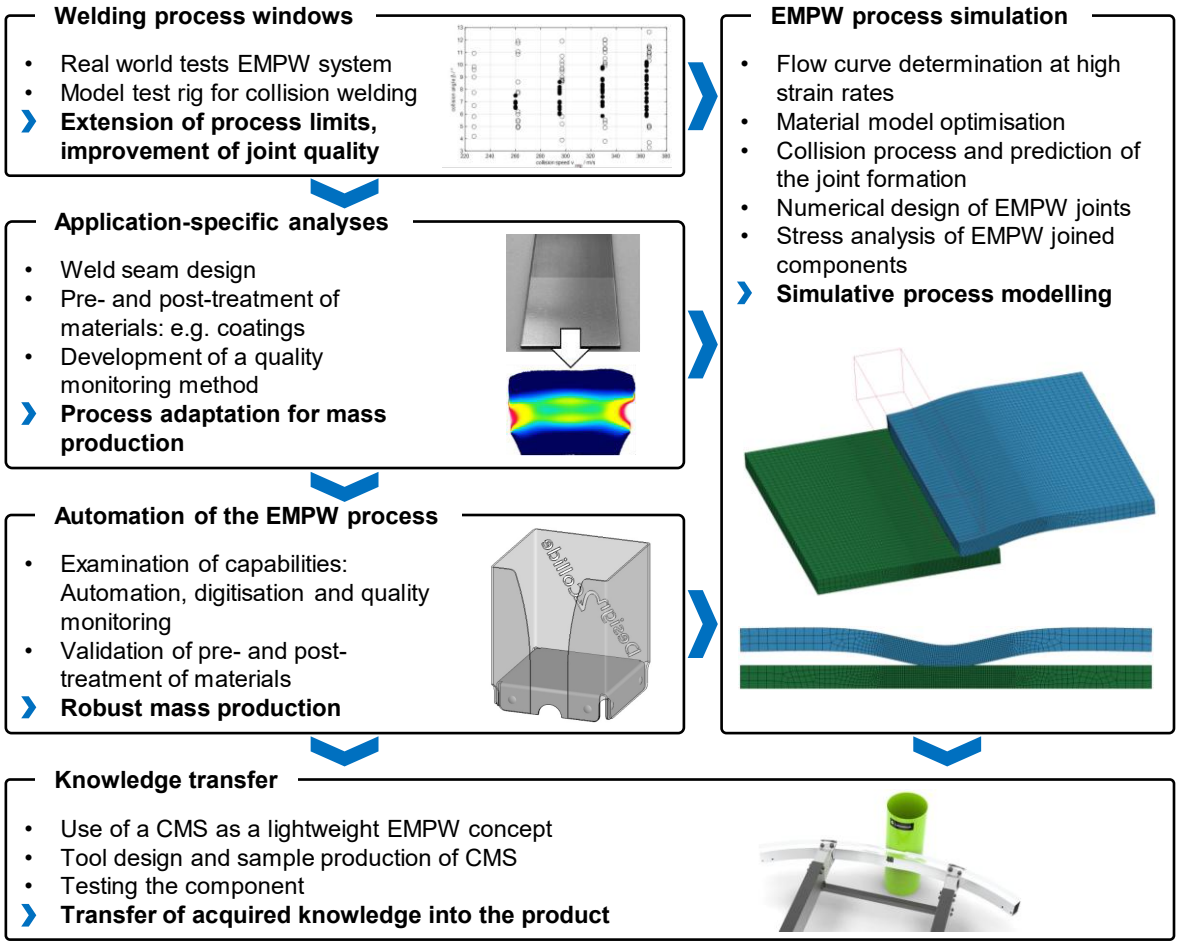

***Figure 1**: Schematic project flow of the Design2Collide research project*

2.1 EMPW-compliant component design

The investigation of EMPW in an industrial environment is based on an established assembly consisting of two elements to be joined together. This assembly is undergoing adaptation for the EMPW. This adaptation includes the material selection, the design consideration of the acceleration gap and ensuring the damage-free formability of the component during the EMPW. A note box consisting of a base and a wall plate is selected as a representative component. The existing note box is manufactured from aluminium using semi-tubular rivets.

2.2 Investigation of collision welding with AA6016 and DC04

Welding tests are carried out on the material combination of AA6016 and DC04 using a model test rig for collision welding and an EMPW system to determine the EMPW parameters and to ensure the best possible joint design for the note box. The model test rig for collision welding, developed at the Institute for Production Engineering and Forming Machines (PtU) at the Technical University of Darmstadt, allows the collision welding

process to be investigated over the time profile of the collision with constant and precisely adjustable collision parameters thanks to its fully mechanical design. It is being used to determine the influences of the collision angle and the collision velocity on the joint formation and the weld seam quality. A detailed description of the test rig is given in (Kraus et al., 2024). The specimens used are taken from DC04 sheets (thickness *t*: 2.0 mm, tensile strength R_m: 310 N/mm^2) and AA6016-T4 sheets (thickness *t*: 2.0 mm, tensile strength R_m: 240 N/mm^2) by shear cutting. The tensile strength values mentioned are determined by performing three tensile tests on a *Zwick Roell 100* combined tensile and compression testing machine in accordance with DIN 50125. The process window is determined by varying collision velocity v_{imp} and collision angle β. The collision velocity is varied in five steps of 227 m/s, 262 m/s, 297 m/s, 331 m/s and 366 m/s by rotating the rotors at a specified frequency. The collision angle is varied between 3° and 13°. The specimens are cleaned with acetone immediately prior to testing to eliminate any influence on the test results from lubricant or corrosion inhibitor residues on the specimen surfaces. High-speed observation of the collision is performed using a *PCO hsfc pro* image intensifier camera, which acquires up to eight images per collision with an exposure time of 20 ns.

The EMPW process parameters are determined by experiments using a *PS48-16* EMPW system from the manufacturer *PSTproducts GmbH* and a coil with an effective area of 80 mm x 10 mm, with particular focus on the acceleration gap before welding, the discharge current and the weld seam design. The gap is analysed in two increments of 1 mm and 1.5 mm. The discharge current is analysed in three steps within a range of 424 kA to 483 kA. In this study, two weld seam designs are analysed, resulting from either a symmetric or an asymmetric collision. In an asymmetric collision, the flyer is only supported on one side. This results in a one-directional collision when it collides with the target. This creates a semi-elliptical weld seam. However, in the case of a symmetrical collision, the flyer is supported on both sides and moves in a rolling motion in both directions from the point of impact, creating an elliptical weld seam. The sheets used are 2.0 mm thick for DC04 (tensile strength R_m: 310 N/mm^2) and 1.5 mm thick for AA6016-T4 (tensile strength R_m: 235 N/mm^2).

2.3 Conversion of the automation system of the robotic production cell

An existing automated modular robotic production cell is modified to be used with a sheet welding tool coil. Irrespective of the actual joining method, the sequence is as follows:

- The two separate parts are manually placed in a workpiece carrier on a rotary table and fed into the production cell via a 180° rotation. Two workpiece carriers are installed on either side of the rotary table.
- The robot simultaneously picks up the note box with a suction pad (base plate) and a pneumatic gripper (wall plate). A sensor for each component is used to check that it is in place. Mechanical provisions ensure precise alignment of the two parts respective to each other.
- The robot moves the box to the joining tool and passes through the three joining positions successively.

- After the last joining operation, the robot places the finished box in the workpiece carrier and picks up a newset of parts.

Two components of the production cell need to be adapted for electromagnetic pulse welding: The riveting station is replaced by the welding unit, which mainly consists of the tool coil. The handling unit on the robot, consisting mainly of the gripper, must be modified so that the electrical components can withstand the electromagnetic field generated by the tool coil. In addition, they must be electrically isolated from the note box in case the insulation of the tool coil is damaged. The core components of the production cell are shown in Fig. 2.

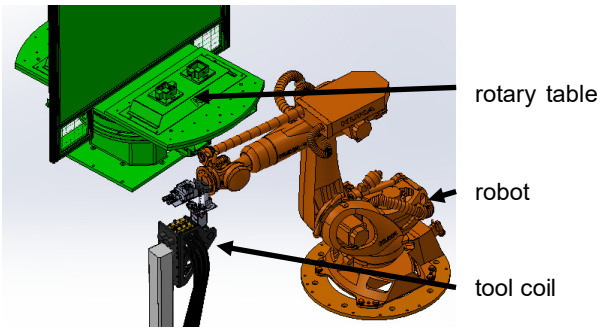

***Figure 2**: Core components of the production cell (the safety fence is not shown).*

2.4 Design of the welding unit

The welding unit consists of the tool coil and the support (or backer) for the target (the base plate of the note box). The effective part of the tool coil, which induces the eddy currents into the workpiece, is the length of the flange of the base plate (83 mm), see Fig. 3 c). With the information from the EMPW examinations (section 3.2), the required peak discharge current is known. The cross-section of the effective part of the tool coil and the number of channels of the pulse generator can be calculated accordingly.

The backer must be able to move by a few millimetres to open the space for the note box to be inserted by the robot. During the welding impact it must be locked in place rigidly. In this closed and locked position, it must be able to withstand the impact of the flyer on the target.

2.5 Post-process quality monitoring

To ensure optimal joint quality, active thermography is utilised as a post-process quality assurance method. The inspection is carried out in a transmission arrangement, with excitation by means of induction. The thermographic system used is a *FLIR SC5600-M*. The technical data of the system are summarized in (Graß et al., 2024). The acquisition frequency is 300 Hz, the integration time is 2 ms and the evaluation time is 0.2 - 5 s after the pulse of the inductor. The evaluation in the frequency domain was carried out at 1.2 Hz. The inductor is cuboidal (80 mm x 70 mm x 65 mm) - the induction parameters are 0.1 s pulse duration, 8 kHz excitation frequency and a pulse width modulation of 470‰. The intention is to generate and detect defective EMPW joints. For this purpose, welding is locally prevented

by the application of an anti-corrosion oil (6 µg/mm²). Defective joining partners should also be taken into account. For this purpose, a joining partner with grooves is prepared before the welding process. To ensure comparability, a reference joint is thermographically analysed. The evaluation is based on the phase images, as these provide the most detailed information on heat transfer.

3 Results

3.1 EMPW-compliant component design

To investigate the automated operation of EMPW and the processes of the associated value chain, an established component, a note box consisting of a wall plate and a base plate, is used and adapted for EMPW. The base plate of the note box will be made of steel (DC04, *t*: 1.5 mm) and the wall plate of aluminium (AA6016, *t*: 1.5 mm). These material adaptations reveal the potential of the EMPW for hybrid aluminium-steel joints. In addition, the choice of aluminium for the wall plate ensures that it can be used as flyer. Fig. 3 shows the note box joined by conventional self-pierce riveting, the note box optimised for the EMPW and a detailed illustration of the joined area. The wall plate of the EMPW note box is welded to the base plate on three sides. The front side of the note box with the opening is left unwelded, as the available areas to be joined are insufficiently large. The EMPW-compliant design of the note box consists mainly of the implementation of eight embossings, ensuring an acceleration gap of 1 mm between the wall and the base plate of the note box. Furthermore, notches are included. These notches ensure the controlled deformation of the wall plate during the acceleration caused by the EMPW.

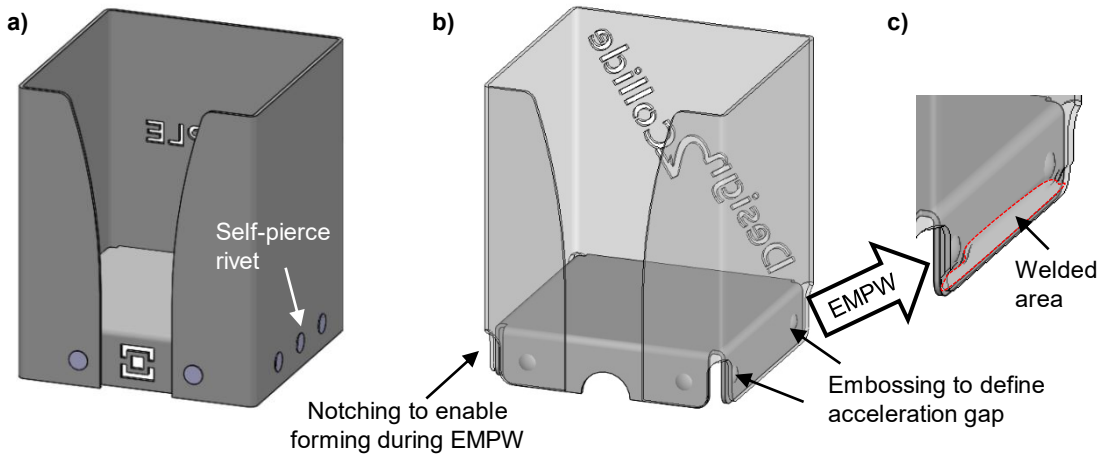

***Figure 3**: a) Conventional note box, joined using self-pierce rivets, b) note box adapted for EMPW c) detail of welded area of note box (flange length 83 mm)*

3.2 Investigation of collision welding with AA6016 and DC04

The welding process window, as determined by using the model test rig for the material combination of aluminium AA6016-T4 (*t*: 2.0 mm) and DC04 steel (*t*: 2.0 mm), is illustrated in Fig. 4. The collision welding tests are performed at collision velocities v_{imp} of 227 m/s, 262 m/s, 297 m/s, 331 m/s and 366 m/s. Within the defined process window, a collision weld test is considered successful if the two specimens cannot be separated by manual force after the test (black dots). To improve the clarity of the diagram, the successful tests are shifted 2 m/s to the left on the collision velocity axis compared to the unsuccessful tests (white dots). The formation of the first bonds between the two materials occurs at a collision velocity of 262 m/s. The lower and upper limit angles at this velocity are 6.5° and 7.5°, respectively. At a collision velocity of 297 m/s, an increased upper limit angle of 8.6° is determined, while the lower limit angle decreases to 6.0°. Furthermore, at collision velocities of 331 m/s and 366 m/s, there is an even greater increase in the upper limit angle to 9.8° and 10.2° respectively, while the lower limit angle decreases marginally to 5.9° for both velocities. More detailed investigations into the relationship between tensile shear strength values and process parameters can be found in (Kraus et al., 2024).

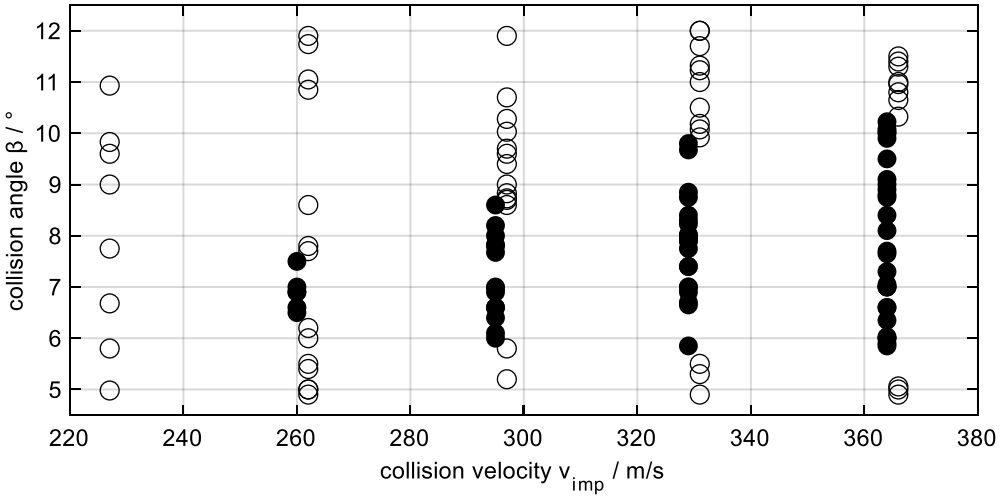

***Figure 4**: Welding process window of AA6016-T4 (flyer) and DC04 (target).*

The investigation of the EMPW of AA6016-T4 (*t*: 1.5 mm) and DC04 (*t*: 2.0 mm) is carried out by examining two different weld designs and varying relevant process parameters. The weld seam designs considered are produced by using a symmetric collision, which results in an elliptical weld seam, see Fig. 5 a), and by forcing an asymmetric collision, which generates a crescent-shaped weld seam (Fig. 5 b). The parameters varied are the acceleration distance and the discharge current. Good joint strengths are obtained using symmetric collision and, in the best case, joints manufactured in this way fail under quasi-static tensile shear stress in the base material. With asymmetric collision, lower joint strengths are achieved in the overall discharge current range under consideration. Nevertheless, it is shown that 1 mm of acceleration gap generates significantly better joint strength than 1.5 mm (Fig. 5 c). The advantage of the symmetrical collision is presumably

due to the larger weld seam. The positive influence of the 1 mm gap is due to its associated effect on the jet. At small collision angles, the jet interacts more strongly with the surfaces of the joining partners and activates them thermally.

The metallographic analysis of the weld seam interface of a joint with symmetrical collision and fabricated with 1 mm acceleration gap shows typical EMPW characteristics. Cracks and pores can be seen at the beginning of the weld seam, compare Fig. 5 d). An EDS (Energy Dispersive X-ray Spectroscopy) line scan (Fig. 5 f) performed through a melt pocket near the beginning of the weld seam shows that oxygen is present. This indicates that parts of the aluminium oxide layer, which is usually ejected as a jet during the plasticisation process during the collision, remained in the interface. The interface at the end of the weld seam also contains localised melt pockets, but these are less prominent than at the beginning of the weld seam (Fig. 5 e). A line scan carried out at the end of the weld seam indicates the absence of oxygen. The chemical composition of the weld seam interface is also influenced by the position of the analysis. In comparison to the EDS line scan of the beginning of the weld seam, lower amounts of iron are detected in the interface, see Fig. 5 g). The differences in the chemical composition are due to the respective collision conditions (collision angle and collision point velocity). Furthermore, the analysed microstructure corroborates the findings regarding the interaction between the mechanical joint strength and the adjusted acceleration distance. The jet interacts with the boundary layers of the joining partners across the entire weld seam area, causing localised melting and resulting in sufficient joint strength.

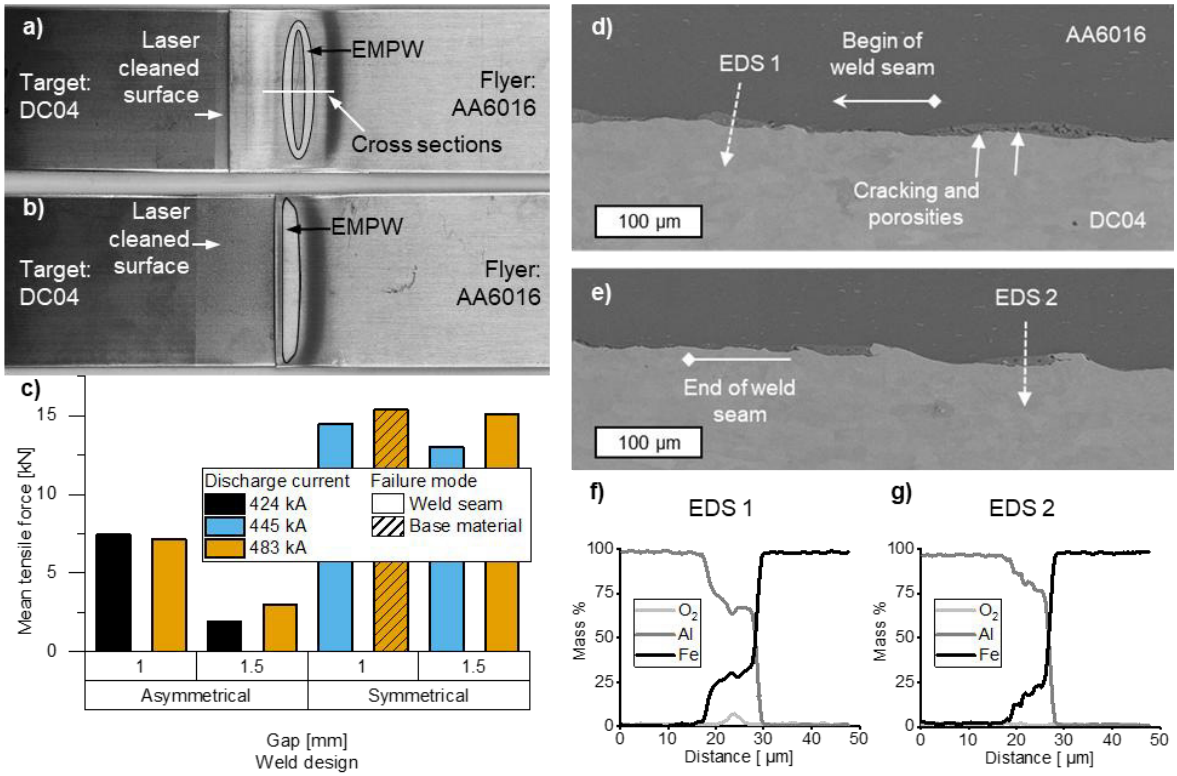

***Figure 5**: AA6016 / DC04 joints: a) symmetrical collision, b) asymmetric collision, c) quasi-static shear tensile strength, d) weld seam (445 kA and 1 mm gap) begin and pos. of EDS scan 1, e) weld seam end and pos. of EDS scan 2, f) EDS 1 line graph, g) EDS 2 line graph*

For the experiments on the note box, the asymmetric collision is chosen despite the inferior mechanical joint properties. The reason for this choice is the accessibility required for the joining and clamping process and the subsequent non-destructive testing.

3.3 Conversion of the automation system of the robotic production cell

The gripper tool and its auxiliary components on the robot are adapted as follows:

- The inductive sensors used for detecting the presence of base and wall plate of the note box are too sensitive to be used near the tool coil due to the electromagnetic fields. They are replaced by optical sensors which effectively measure the same parameter: The distance between the sensor and the workpiece.
- All other electronic components (e.g. the pneumatic valves or the field bus coupler) are moved as far away as possible from the tool coil and the note box to reduce electromagnetic interference.
- If the insulation of the tool coil is damaged, the high voltage can cause a high current to flow into the grounded robot and all attached components. To protect the robot and the electrical components at the hand of the robot, the note box is insulated from all other components by fibre-reinforced plastic parts. An air gap of about 20 mm is sufficient for the maximum charging voltage of 16 kV.
- Eddy currents are minimised by additional layers of insulating material between conductive components. They cut off the path of the eddy currents. These insulations only need to be a few millimetres thick, as the voltage potential of the eddy currents is far lower than the charging voltage.

As a result of these adaptions, almost all other components are modified as a direct consequence.

3.4 Design of the welding unit

The welding unit consists of the tool coil, the backer and its mechanism, and a frame with a mounting flange, see Fig. 6. The assembly will be mounted on a post for ergonomic reasons. The design of the tool coil can be broken down into the effective part, which induces the eddy currents into the workpiece, its support, which absorbs the reaction force, and the clamping for the pulse cables. The length of the effective part of the tool coil is 83 mm, which is given by the dimensions of the note box. Its cross-section is defined as 10 mm x 7 mm according to the estimated maximal peak discharge current of 500 kA. This discharge current value also determines the number of capacitors. In order to have some reserve, a pulse generator with six capacitors is used.

The key requirement for the backer is that it can be moved by a few millimetres and locked in the pulse position. This is fulfilled by a toggle lever operated by a compact pneumatic cylinder. The toggle lever moves a class I lever, multiplying the force by about seven. To withstand the impact forces and absorb as much of the shock load as possible, this lever is designed with as much steel as possible. The area which is in direct contact with the note box is a separate component with a simple geometry, making it cheap and easy to

replace. This also facilitates experimental testing of different materials for this task. The adjustment of the lever is accomplished by shims and by the pneumatic cylinder.

The frame holds both the tool coil and the lever of the backer. It is strong enough to withstand the shock loads on the tool coil and the backer. The position of the tool coil within the frame can be modified for fine tuning. The mounting flange is part of the frame. For electrical safety reasons, the frame is electrically insulated from the post onto which it is mounted.

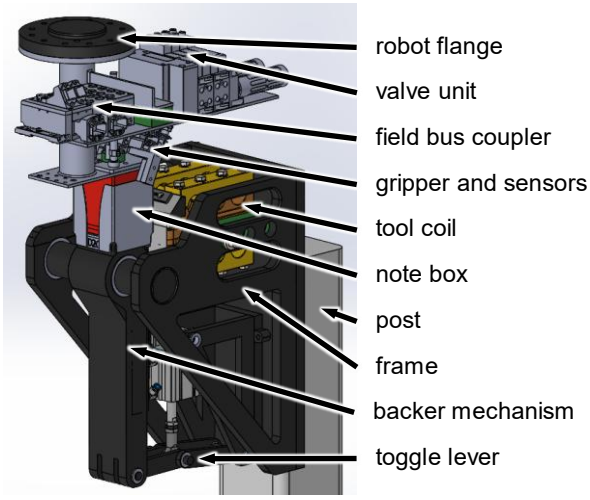

***Figure 6**: Welding unit (tool coil, backer, frame) and robot tool (gripper, valves, field bus coupler)*

3.5 Post-process quality monitoring

EMPW joined specimens are analysed using active thermography. The excitation is carried out inductively and the test setup is a transmission arrangement. Both aspects ensure transferability to investigations on the note box. In addition to a defect-free reference specimen, three specimens with defects are analysed, see Fig. 7. Welding is prevented in the centre and on one side by the selective application of an anti-corrosion oil. Furthermore, three grooves are milled into a DC04 target, which are intended to negatively affect the weld seam formation. All specimens are analysed using phase images. The phase images provide information on the thermal wave characteristics at the specimen surface in relation to time aspects of the excitation.

The phase image of the reference specimen reveals a widespread heat transfer without a large time delay, indicating a consistent weld. The application of an anti-corrosion oil results in incomplete welding and inhibits heat transfer from the target to the flyer. This is shown in Fig. 7 b) and c). It is clearly recognisable that heat transfer occurs only off-centre or on one side of the specimen. The influence of grooves on the heat transfer from the target to the flyer is also visible. This results in an inconsistent time delay of the heat wave relative to the excitation. This can be perceived as hotspots whose positions correspond to those of the grooves, compare Fig. 7 d).

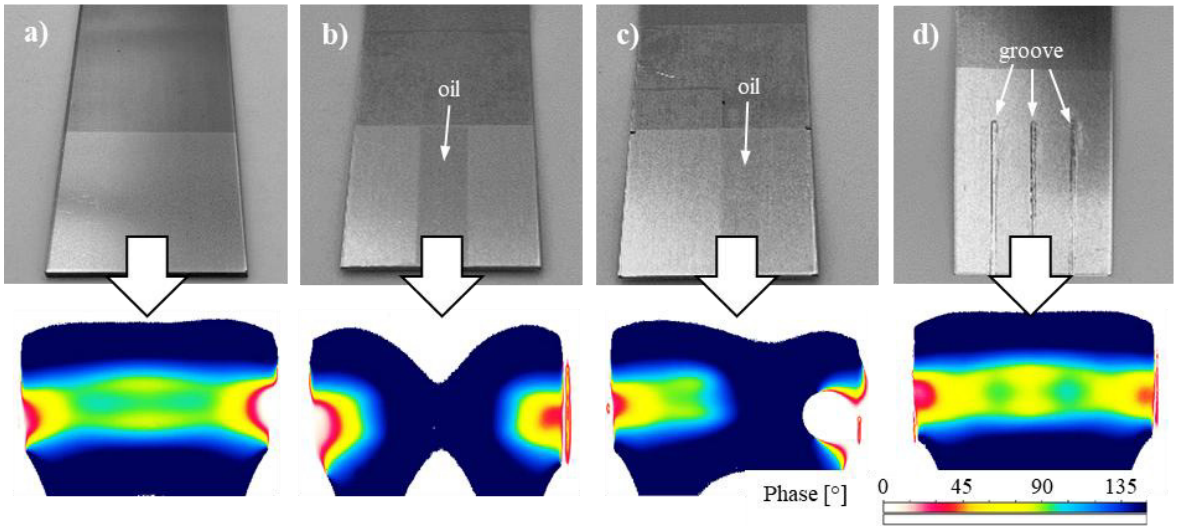

***Figure** 7: Images of samples and corresponding phase images of a) a reference joint, b) a joint with a central defect, c) a joint with a off-centre defect, d) a joint with three grooves*

4 Summary

In the present study, EMPW was examined in the broader context of industrial application, with particular emphasis on the fundamental steps in the value chain. A suitable existing demonstration component, namely a note box, is used to show how a redesign according to EMPW can be achieved. The selection of materials is an integral part of this process. The materials selected for this project are aluminium AA6016-T4 and steel DC04, which are successfully joined after preliminary investigations using a model test rig and an EMPW system. Interactions between process and collision parameters and the joint properties are also demonstrated. Additionally, a tool coil and handling concept are developed to enable the automated production of the demonstration component. A quality monitoring process based on active thermography is investigated to ensure joint quality. Using joints fabricated by EMPW, it is demonstrated that the presence of defective welds can be detected through the analysis of phase images.

5 Outlook

In the further course of the research project, the results and measures presented in this paper will be transferred into a functional process for the automated production of the note box. The process will then be evaluated for robustness and reproducibility with regard to mass-production of EMPW joined multi-material aluminium and steel components. The effects of selected upstream and downstream material treatments, such as corrosion prevention and passivation systems, on the welding result are also being investigated using the EMPW system and the model test rig. These material treatments represent, for example, alternatives to current corrosion prevention systems such as zinc plating or anti-corrosion oils, which prevent welding with EMPW and require additional costly process steps (e.g. surface

cleaning, removal of the zinc layer) in an industrial environment. The results will also be validated using the automated process.

In the area of process simulation, material models are being optimised with already determined flow curves for various aluminium and steel materials at high strain rates. These models will be used to more accurately simulate the EMPW collision process to enable predictions of joint formation in relation to the process windows determined by the model test rig. This will enable the simulation-based design of EMPW welds and, based on this, the numerical stress analysis of EMPW welded components. The physical and virtual design results are then combined and used for the targeted design and manufacture of a product. A lightweight Crash Management System (CMS) for light vehicles has already been selected as the product to demonstrate the performance of the EMPW joints. The CMS is required to withstand a wide range of different load collectives, both in normal operation and in the event of a crash. The successful implementation of the product design will be validated by load tests of physically manufactured CMS.

Funding

This research is a result of the project Design2Collide – Kollisionsgeschweißte Hybrid-Leichtbaustrukturen. The project is funded by the Federal Ministry for Economic Affairs and Energy (BMWE, 03LB5008A-H), based on a decision taken by the German Bundestag. The authors are solely responsible for the content in this publication.

References

Agudo, L., Eyidi, D., Schmaranzer, C.H., Arenholz, E., Jank, N., Bruckner, J., Pyzalla, A.R., 2007. *Intermetallic Fe_xAl_y-phases in a steel/Al-alloy fusion weld*. Journal of Materials Science 42, pp. 4205-4214.

Atabaki, M.M., Nikodinovski, M., Chenier, P., Ma, J., Harooni, M., Kovacevic, R., 2014. *Welding of Aluminum Alloys to Steels: An Overview*. Journal for Manufacturing Science and Production 14, pp. 59-78.

Bandivadekar, A., Bodek, K., Cheah, L., Evans, C., Groode, T., Heywood, J., Kasseris, E., Kromer, M., Weiss, M., 2008. On the Road in 2035: Reducing Transportation's Petroleum Consumption and GHG Emissions. Cambridge, MA, USA. Available online: http://web.mit.edu/sloan-auto-lab/research/beforeh2/otr2035/ (accessed on 10 May 2024).

Beddows, D.C.S., Harrison, R.M., 2021. *PM10 and PM2.5 emission factors for non-exhaust particles from road vehicles: Dependence upon vehicle mass and implica-tions for battery electric vehicles*. Atmospheric Environment 244, 117886.

Carlone, P., Astarita, A., 2019. *Dissimilar Metal Welding*. Metals 9, 1206.

Crippa, M., Guizzardi, D., Pagani, F., Banja, M., Muntean, M., Schaaf, E., Monforti-Ferrario, F., Becker, W., Quadrelli, R., Risquez Martin, A., Taghavi-Moharamli, P., Köykkä, J., Grassi, G., Rossi, S., Melo, J., Oom, D., Branco, A., San-Miguel, J.,

Manca, G., Pisoni, E., Vignati, E., Pekar, F, 2024. GHG Emissions of all World Countries, Publications Office of the European Union, Luxembourg.

EDGAR (Emissions Database for Global Atmospheric Research), 2024. IEA-EDGAR fossil CO_2 emissions. Available online: https://edgar.jrc.ec.europa.eu/report_2024#data_download (accessed on 07 April 2025).

Graß, M., Sommer, N., Böhm, S., 2024. *Enabling magnetic pulse welding for dissimilar tubular arrester cable joints*. Welding in the World 68, pp 1837-1852.

IEA, 2025. Global total final consumption by fuel in the Net Zero Scenario, 2010-2050, Paris, France. Available online: www.iea.org/data-and-statistics/charts/global-total-final-consumption-by-fuel-in-the-net-zero-scenario-2010-2050 (accessed on 07 April 2025).

Kapil, A., Sharma, A., 2015. *Magnetic pulse welding: An efficient and environmentally friendly multi-material joining technique*. Journal of Cleaner Production 100, pp. 35-58.

Khedr, M., Hamada, A., Järvenpää, A., Elkatatny, S., Abd-Elaziem, W., 2023. *Review on the Solid-State Welding of Steels: Diffusion Bonding and Friction Stir Welding Processes*. Metals 13, 54.

Kraus, S.O., Bruder, J., Groche, P., 2024. *The Influence of Weld Interface Characteristics on the Bond Strength of Collision Welded Aluminium-Steel Joints*. Materials 17, 3863.

Lopez, B., Wang, X., Chen, L.W.A., Ma, T., Mendez-Jimenez, D., Cobb, L.C., Frederickson, C., Fang, T., Hwang, B., Shiraiwa, M., Park, M., Park, P., Yao, Q., Yoon, S., Jung, H., 2023. *Metal contents and size distributions of brake and tire wear particles dispersed in the near-road environment*. Science of The Total Environment 883, 163561.

Marschner, O., Pabst, C., Schäfer, R., Pasquale, P., 2021. Suitable Design for Electromagnetic Pulse Processes. In: High Speed Forming 2021, Proceedings of the 9th International Conference, Dortmund, Germany, pp. 1-9.

Organisation for Economic Co-Operation and Development (OECD) The International Transport Forum, 2017. Lightening Up: How Less Heavy Vehicles Can Help Cut CO2 Emissions. Available online: https://www.itf-oecd.org/less-heavy-vehicles-cut-co2-emissions (accessed on 07 April 2025).

Timmers, V.R.J.H., Achten, P.A.J., 2016. *Non-exhaust PM emissions from electric vehicles*. Atmospheric Environment 134, pp. 10-17.

Tisza, M., Lukács, Z., 2018. *High strength aluminum alloys in car manufacturing*. IOP Conference Series: Materials Science and Engineering 418, 012033.